



miR-29c&b2 encourage extramedullary infiltration resulting in the poor prognosis of acute myeloid leukemia

Yanyu Wei¹ · Wei Lu¹ · Yehua Yu¹ · Yuanmei Zhai² · Hezhou Guo¹ · Shaoxin Yang¹ · Chong Zhao¹ · Yanjie Zhang¹ · Jiali Liu¹ · Yuhui Liu³ · Jian Fei^{3,4} · Jun Shi¹

Received: 30 September 2020 / Revised: 11 March 2021 / Accepted: 29 March 2021 / Published online: 22 April 2021
© The Author(s), under exclusive licence to Springer Nature Limited 2021

Abstract

Extramedullary infiltration (EMI), as a concomitant symptom of acute myeloid leukemia (AML), is associated with low complete remission and poor prognosis in AML. However, the mechanism of EMI remains indistinct. Clinical trials showed that increased miR-29s were associated with a poor overall survival in AML [14]. Nevertheless, they were proved to work as tumor suppressor genes by encouraging apoptosis and inhibiting proliferation in vitro. These contradictory results led us to the hypothesis that miR-29s may play a notable role in the prognosis of AML rather than leukemogenesis. Thus, we explored the specimens of AML patients and addressed this issue into miR-29c&b2 knockout mice. As a result, a poor overall survival and invasive blast cells were observed in high miR-29c&b2-expression patients, and the wildtype mice presented a shorter survival with heavier leukemia infiltration in extramedullary organs. Subsequently, we found that the miR-29c&b2 inside leukemia cells promoted EMI, but not the one in the microenvironment. The analysis of signal pathway revealed that miR-29c&b2 could target HMG-box transcription factor 1 (Hbp1) directly, then reduced Hbp1 bound to the promoter of non-muscle myosin IIB (Myh10) as a transcript inhibitor. Thus, increased Myh10 encouraged the migration of leukemia cells. Accordingly, AML patients with EMI were confirmed to have high miR-29c&b2 and MYH10 with low HBP1. Therefore, we identify that miR-29c&b2 contribute to the poor prognosis of AML patients by promoting EMI, and related genes analyses are prospectively feasible in assessment of AML outcome.

Supplementary information The online version contains supplementary material available at <https://doi.org/10.1038/s41388-021-01775-9>.

✉ Jian Fei
jfei@tongji.edu.cn

✉ Jun Shi
junshi@sjtu.edu.cn

¹ Department of Hematology, Shanghai Ninth People's Hospital, Shanghai Jiaotong University School of Medicine, Shanghai, China

² Department of Hematology, Tongren Hospital, Shanghai Jiaotong University School of Medicine, Shanghai, China

³ School of Life Science and Technology, Tongji University, Shanghai, China

⁴ Shanghai Engineering Research Center for Model Organisms, SMOC, Shanghai, China

Introduction

Acute myeloid leukemia (AML) is a malignant clonal disease originating in bone marrow (BM), from which invasive myeloblasts spread to peripheral blood (PB). It is well known that the chemotherapy resistance, tumor microenvironment, and tumor cells themselves are related to the outcome of AML [1–4]. However, extramedullary infiltration (EMI), as a common concomitant symptom of AML, is part of the initial diagnosis in about 30% of AML patients [5–8], little attention has been paid to it. Recent studies have reported that EMI leads to a poor outcome in both adults and children with leukemia [6, 9, 10], but researchers tend to regard EMI simply as a common concomitant symptom as leukemia cells can spread to multiple extramedullary systems through blood vessels. The underestimation has led to a lack of studies on the mechanism of EMI. Only a few studies showed that DNMT3A and CD56 participated in the process of EMI [6, 11]. Thus, the mechanism research of EMI remains indistinct.

As non-coding RNAs, miRNAs are found related to metastasis. miR-29s usually work as tumor suppressors in AML by inhibiting the proliferation or promoting the apoptosis of leukemia cells *in vitro* [12, 13]. But clinical studies show that higher miR-29c contributes to poor prognosis in leukemia patients [14], leading us to suspect that miR-29s might impact the outcome of AML in other ways. Meanwhile, it is reported that miR-29s can influence the invasion of solid tumor by affecting extracellular matrix and angiogenesis [15–18]. It is known that miRNAs regulate the expression of a variety of genes, and their exact roles in a tumor are determined by the dynamic between various biological functions [19]. These facts, combined with the contradictory results of miR-29s in AML and their roles in the metastasis of solid tumors, lead us to the hypothesis that the dominant role of miR-29s is promoting EMI in AML, which results in adverse prognosis.

In this paper, we explored this hypothesis through studying AML patients combined with miR-29c&b2 knockout mice. The study revealed that miR-29c&b2 enhanced the motility of leukemia cells through HBP1/MYH10 axis, which encouraged the EMI, leading to the poor prognosis in AML. In addition to improving our understanding of EMI's cellular processes and pathogenesis, these findings also provide a new approach to the assessment of AML.

Results

miR-29c&miR-29b2 were related to poor outcome and severe EMI in AML

We downloaded gene expression profiles and clinical information of AML patients with initial pathologic diagnosis from the TCGA database. The survival analysis showed that both miR-29c and miR-29b2 were related to poor outcome in AML (Fig. 1A). Analysis on several standard AML clinical risk factors showed no difference among different groups, which also demonstrated that the expression of miR-29c&b2 remained prognostically significant (Supplementary Fig. S1A). Meanwhile, fewer blast cells were observed in BM of higher miR-29c&b2-expression patients (Fig. 1B), while there was no difference in blast cell counts of PB (Fig. 1C).

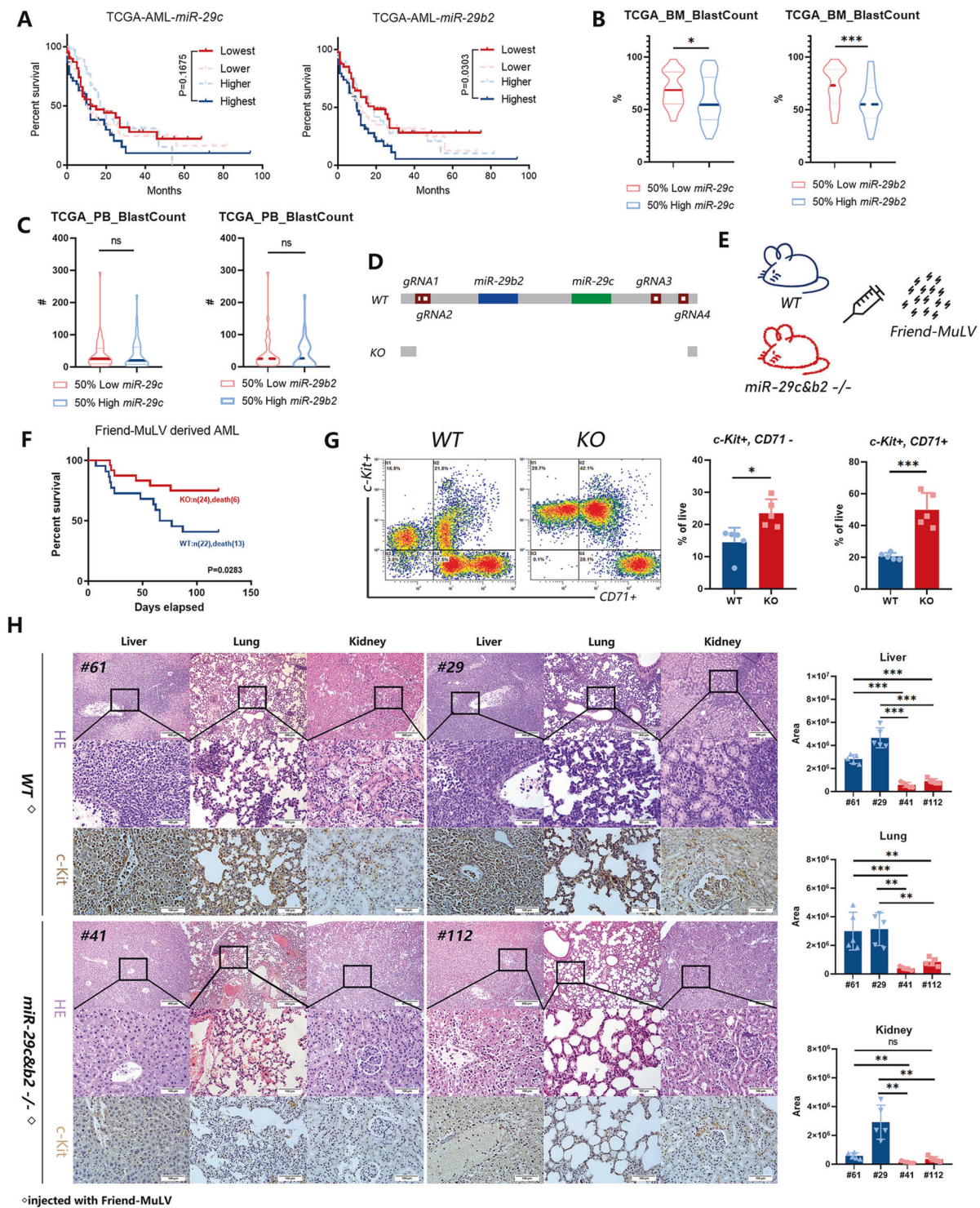
We then evaluated the potential function of miR-29c&b2 on AML by knocking out miR-29c&b2 in C57 mice (Fig. 1D). Friend-MuLV, secreted by FBL-3 cells (a mouse leukemia cell line), was injected into miR-29c&b2^{-/-} or wildtype (WT) mice to induce erythroleukemia (Fig. 1E) [20–22]. Leukemia cells could be observed in PB around day 21 in both groups (Supplementary Fig. S1B). The survival analysis showed that miR-29c&b2^{-/-} mice had a

better prognosis, and the mortality was 34% lower than WT mice (Fig. 1F). Strikingly, flow-cytometric analysis of BM showed that percentage of the myeloblast (c-Kit⁺, CD71⁻) and proerythroblast (c-Kit⁺, CD71⁺) was higher in BM of miR-29c&b2^{-/-} mice (Fig. 1G), indicating a heavier leukemia burden in BM of miR-29c&b2^{-/-} mice than in WT mice. Meanwhile, the hematopoiesis made no difference in most of the time, and there were similar blast cell counts in PB between two groups right before the conclusion of the experiment (Supplementary Fig. S1C, D). These conflicting results between BM and PB suggested that miR-29s might enhance the infiltration of leukemia cells, leading to poor prognosis. To explore EMI in mice, tissues were collected after mice deceased. More leukemia clusters were found in the WT mice's extramedullary organs, such as livers, kidney, and lungs (Fig. 1H and Supplementary Fig. S1E). Together, these results proved that miR-29c&b2 encouraged EMI, which might be the reason behind shorter survival and increased mortality.

miR-29c&b2 in leukemia cells encouraged the EMI

Since miR-29c&b2 were knocked out conventionally in C57 mice, we were unable to define whether it was the miR-29c&b2 in microenvironment or leukemia cells that promoted the EMI. Therefore, wild-genotype FBL-3 cells with GFP were injected into miR-29c&b2^{-/-} and WT mice, respectively (Fig. 2A). Neither overall survival nor EMI contributed to a difference between two groups (Fig. 2B, C and Supplementary Fig. S2A). The percentage of FBL-3 cells in BM also made no difference (Supplementary Fig. S1B). The results above indicated that miR-29c&b2 in microenvironment was not responsible for the AML EMI or the leukemia burden in BM.

Subsequently, the cross-transplantation was conducted to evaluate the impact of miR-29c&b2 in leukemia cells. FBL-3 cells with miR-29c/b2 knocked out by CRISPR/Cas9 were injected into WT mice, while WT FBL-3 cells were injected into miR-29c&b2^{-/-} mice (Fig. 2D). As a result, WT mice had a higher median overall survival and less mortality than miR-29c&b2^{-/-} mice (Fig. 2E). As expected, the infiltration of leukemia clusters in miR-29c&b2^{-/-} mice was more severe than WT mice (Fig. 2F and Supplementary Fig. S2C), while the white blood cells in PB made no difference between two groups (Supplementary Fig. S2D). The percentage of miR-29c&b2^{-/-} FBL-3 cells was higher than WT FBL-3 cells in BM, but there was no difference on total cell counts (Supplementary Fig. S2E). The homing assays also showed that miR-29c&b2^{-/-} FBL-3 cells migrated into marrow less than WT FBL-3 cells (Supplementary Fig. S2F). To confirm the effect of miR-29c&b2 in AML cells, the phenotypes above were conducted by other AML models of C1498 or



MV4-11 (Supplementary Fig. S3). These results revealed that miR-29c&b2 in leukemia cells might contribute to the EMI of AML. Indeed, the migration of leukemia cells was proved to be regulated by miR-29c&b2 in vitro (Fig. 2G, H). On the other side, the clone formation assays, cell growth assays, and the differentiation analysis of AML

cells showed that miR-29c&b2 suppressed cell growth moderately (Supplementary Fig. S4A–C) and did not regulate the differentiation of AML cells (Supplementary Fig. S4D, E). All factors considered, it was the EMI induced by miR-29c&b2 in leukemia cells that contributed to a poor outcome in AML mice.

◀ **Fig. 1 miR-29c&miR-29b2 were related to poor outcome and severe EMI in AML.** **A** Excluding subtype M3, patients with AML in TCGA database were divided into four groups equally by miR-29c or miR-29b2 expression and the overall survival was analyzed. Statistical significance was evaluated by log-rank test. **B, C** The analysis of BM or PB blast cell counts of AML patients in TCGA database (patients with subtype M3 or who had previously undergone chemotherapy were excluded). Patients were stratified by miR-29c or miR-29b2 expression into 50% high ($n = 40$) and 50% low ($n = 40$). **D** The scheme describes miR-29c&b2 knockout strategy in mice by CRISPR/Cas9. **E** The scheme describes the experiment. **F** Survival curve of the miR-29c&b2 $^{-/-}$ mice ($n = 24$; median survival, undefined) and WT mice ($n = 22$; median survival, 71.6 days). **G** Representative flow cytometry profiles and quantification of the frequencies of the myeloblast (c-Kit $^{+}$, CD71 $^{-}$) and proerythroblast (c-Kit $^{+}$, CD71 $^{+}$) in the BM of the dead mice. **H** H&E staining and IHC of c-Kit $^{+}$ of the liver, lung, kidney of the miR-29c&b2 $^{-/-}$ mice (#41, died at day 44; #112, died at day 76) and WT mice (#61, died at day 48; #29, died at day 77), with the quantitatively analysis of IHC sections. All results are representative of at least three independent experiments.

miR-29c/miR-29b2-3p contributes to the migration of AML cells by suppressing Hbp1

To identify candidate mRNAs regulated by miR-29c&b2-3p that promote EMI, we queried three publicly available databases (Target Scan, microRNA.org, and miRDB.org), cataloged mRNAs predicted (Supplementary Fig. S5A) which met the criteria and investigated these mRNAs for their known relevance to cancer biology. Among them, high mobility group box (HMG-box) transcription factor 1 (Hbp1) was found related to the better prognosis of AML patients in TCGA database. Compared to the lower group, AML patients with higher expression of HBP1 underwent a longer overall survival (Fig. 3A). As predicted, miR-29c-3p and miR-29b2-3p might target identical sequences in the Hbp1 3'UTR with the same seed sequence (Fig. 3B). To verify this, we cloned the Hbp1 3'UTR into pmirGLO-REPORTTM vector and mutated the predicted binding site (Fig. 3C). Dual-luciferase assays demonstrated that activity of luciferase with Hbp1 3'UTR could be regulated by miR-29c-3p or miR-29b2-3p. In addition, the regulation was ineffective in the Hbp1 3'UTR mutant group (Fig. 3D). These findings implied that miR-29c&b2-3p were capable of targeting Hbp1 by the identical sequences predicted.

To further confirm this pathway in leukemia cells, we introduced mimics or inhibitors of miR-29c/b2-3p in FBL-3 cells. The western blotting analysis showed that Hbp1 expression decreased after adding mimics of miR-29c/b2-3p and increased by inhibiting the miR-29c/b2-3p (Fig. 3E). Subsequently, FBL-3 cells were infected with lentivirus carrying short-hairpin RNA (shRNA) designed to target Hbp1 specifically. Compared to a non-silencing control, the shRNA mediated downregulation of Hbp1 transcript and protein (Fig. 3F, G). On the other hand, the western blotting analysis showed that Hbp1 expression could be rescued by

transfecting the inhibitors of miR-29c/b2-3p (Fig. 3I). These observations confirmed that miR-29c&b2-3p target Hbp1 in leukemia cells.

Transwell analysis identified the role of Hbp1 in regulating the migration of leukemia cells. Results showed that the Hbp1 downexpressed cells migrated more when compared to the control cells (Fig. 3H), which could also be reversed by introducing inhibitors of miR-29c/b2-3p (Fig. 3J). However, due to the ceiling effect, there was no difference in 167 cell migration (Supplementary Fig. S5D, E) after overexpressing the Hbp1 in FBL-3 cells (Supplementary Fig. S5B, C). Similarly, the immunohistochemistry analysis showed a higher expression of Hbp1 in BM of miR-29c&b2 $^{-/-}$ mice when compared to WT mice (Fig. 3K). These findings suggested that Hbp1 was a target of miR-29c&b2-3p and suppressed cell migration in AML.

Hbp1 mediates the transcription of Myh10

As a transcription repressor, Hbp1 influenced cellular functions by regulating the transcription of other genes. The analysis of RNA-seq with c-kit $^{+}$ cells in BM of leukemic mice showed that Myh10 ranked high among all the differential genes and ranked top in the list of genes that regulated cell motility (Table 1 and Fig. 4A). And the evaluation of HSC/LSC and erythroid differentiation-related gene sets were provided (Table 2). Also, the correlation analysis in the TCGA database implied a positive correlation between miR-29c/b2 and MYH10, which suggested that Myh10 might have played a vital role (Supplementary Fig. S6A). The potential binding site in the promoter of Myh10 was first predicted by Jasp database (Fig. 4B). Then ChIP-PCR assay verified that Hbp1 could bind with the predicted sequence of Myh10 promoter (Fig. 4C). Subsequently, we cloned and inserted repeats of the predicted binding site (bs) in pmirGLO-REPORTTM vector. Sequences of Hbp1-202 and Hbp1-201, the latter lacking HMG-box domain, were cloned into pGFP-N1 vector (Supplementary Fig. S6B). The dual-luciferase assay demonstrated that Hbp1-202 could suppress luciferase expression of pmirGLO-6xbs-REPORTTM vector comparing to the original vector, while Hbp1-201, which lacks HMG-box domain, had no suppressing effect (Fig. 4D). It was also confirmed that the 508 bp before the exons of Myh10 contained the core promoter (Supplementary Fig. S6C, D). The results above showed that Hbp1 could bind to the promoter of Myh10 by its HMG-box domain and suppress the transcription of Myh10. Although the overexpression of Hbp1 was unable to suppress Myh10 due to the ceiling effect (Supplementary Fig. S6E), the expression of Myh10 was enhanced in FBL-3 cells with shHbp1 (Supplementary Fig. S6F–H) or mimics of miR-29c/b2-3p, while it was suppressed when transfected with inhibitors

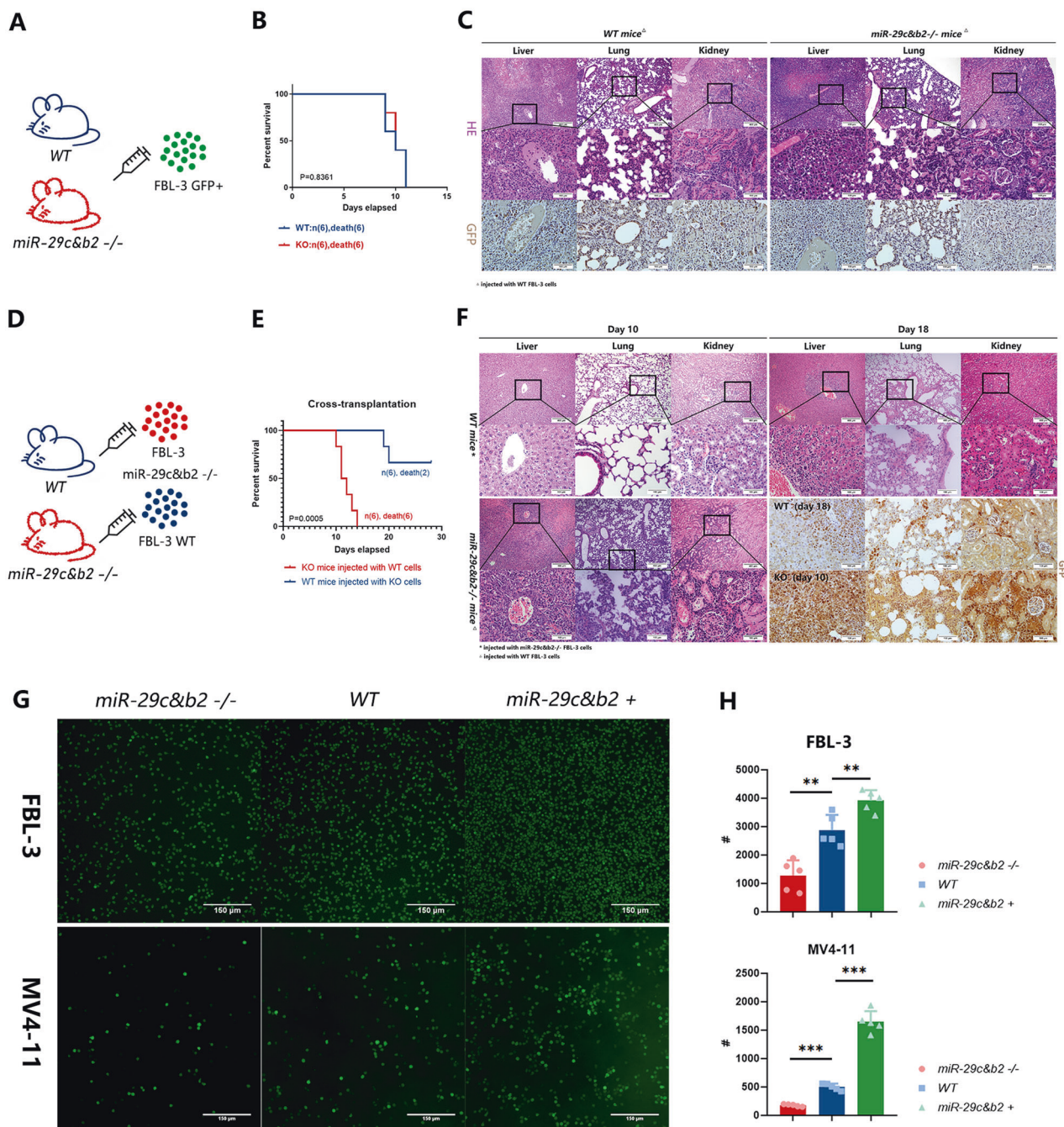
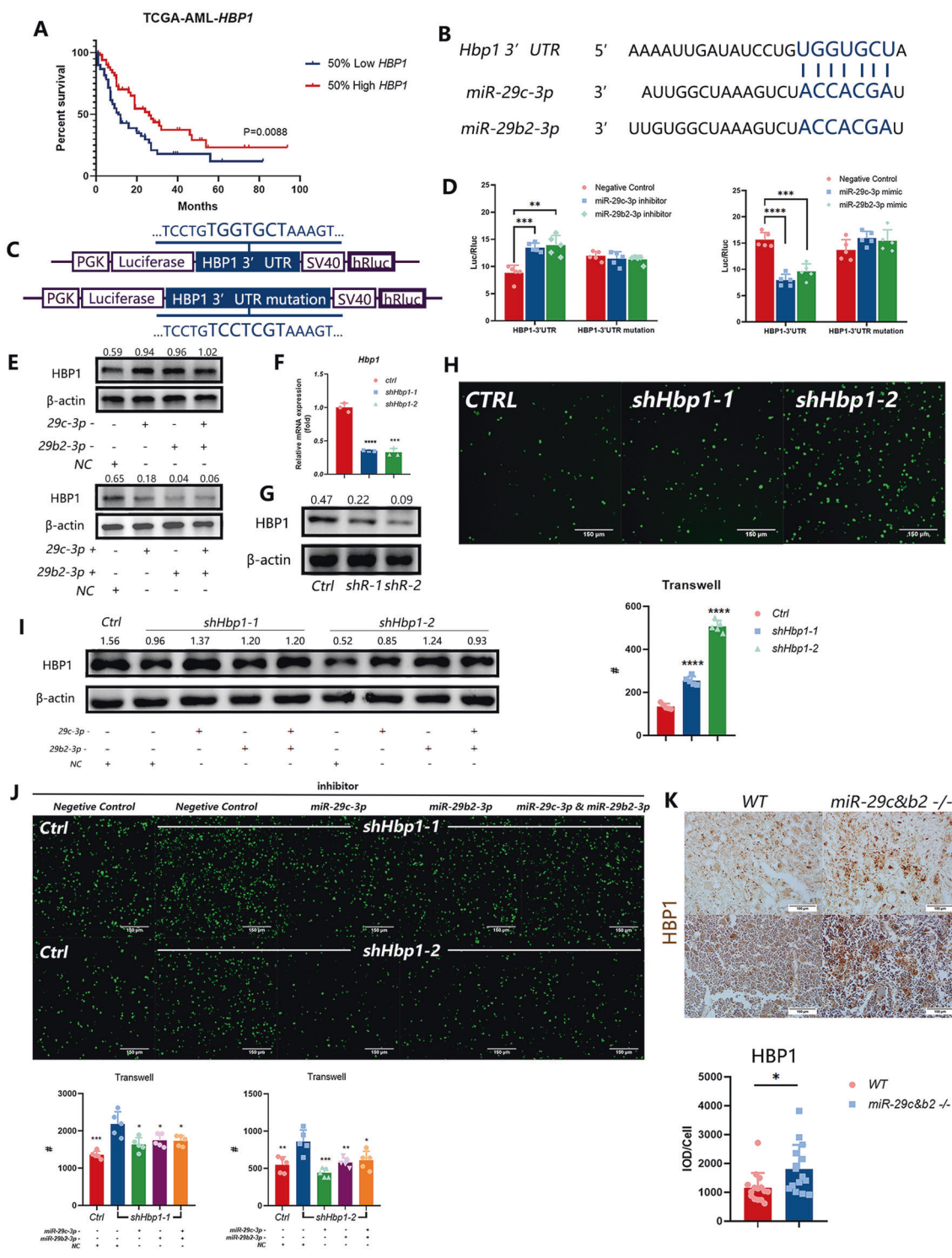


Fig. 2 miR-29c&b2 in leukemia cells encouraged the EMI. **A, D** The scheme describes the experiment. **B** Survival curve of the miR-29c&b2^{-/-} mice ($n = 6$; median survival, 10 days) or WT mice ($n = 6$; median survival, 10 days) that underwent FBL-3 GFP⁺ cells transplantation, representative of three independent experiments. **C** Livers, lungs, and kidneys of these mice died at day 10 after injection were subjected to H&E staining and IHC of GFP⁺. **E** Survival curve of the miR-29c&b2^{-/-} mice ($n = 6$; median survival, 11.5 days) that underwent FBL-3 GFP⁺ cells transplantation or WT mice ($n = 6$;

median survival, undefined) that underwent miR-29c&b2^{-/-} FBL-3 cells transplantation, representative of three independent experiments. **F** Livers, lungs, and kidneys of these mice died at day 10 or 18 after injection were subjected to H&E staining and IHC of GFP⁺. **G, H** The miR-29c&b2^{-/-} FBL-3/MV4-11, WT FBL-3/MV4-11, and miR-29c&b2⁺ FBL-3/MV4-11 cells were subjected to transwell migration assays. All results are representative of at least three independent experiments.

(Supplementary Fig. S6I–K). These findings demonstrated that miR-29c&b2 and Hbp1 could regulate the expression of Myh10 in FBL-3 cells.

Expression of Myh10 was knocked down in FBL-3 cells to explore its effect on migration (Fig. 4E, F). Transwell assays showed that FBL-3 cells with lower Myh10 migrated



less (Fig. 4G). As expected, shHbp1 and miR-29c&b2 mimics could rescue the expression of Myh10 in Myh10 knock down cells (Fig. 4H, I, K, L). The reduction in migration, which resulted from lower expression of Myh10, could also be rescued (Fig. 4J, M). Compared to WT mice,

miR-29c&b2^{-/-} mice showed lower protein expression of Myh10 in BM, (Fig. 4N). These findings proved that Myh10, a non-muscle myosin, controlled the migration of leukemia cells and miR-29c&b2 contributed to the EMI of AML by Hbp1/Myh10 axis.

Fig. 3 miR-29c/miR-29b2-3p contributes to the migration of AML cells by suppressing Hbp1. **A** Overall survival of patients with AML (subtype M3 excluded) from TCGA database was stratified by HBP1 expression into 50% low ($n = 64$; median survival, 10.98 months) and 50% high ($n = 64$; median survival, 25.97 months) groups. Statistical significance was evaluated by log-rank test. **B** Alignment of the miR-29c/b2-3p seed sequence with the Hbp1 3' UTR. Dashed lines represent complementary base pairing. **C** The scheme describes the building strategy of dual-luciferase-reporter vectors with Hbp1 3'UTR or the mutant. **D** Luciferase expression in 293T cells, which were transfected with pmirGLO-REPORTTM vector containing the Hbp1 3'UTR or Hbp1 3'UTR mutant and treated with miR-29c/b2-3p mimic/inhibitor or a scrambled mimic/inhibitor. Renilla luciferase activity was used as a reference. **E** HBP1 protein expression after miR-29c/b2-3p mimic/inhibitor or a scrambled mimic/inhibitor infection in FBL-3 cells. Equivalent gel loading was confirmed by probing with antibodies against β -actin. **F–H** Hbp1 RNA (**F**) or protein (**G**) expression of FBL-3 stably expressing Ctrl or shHbp1-1 or shHbp1-2. Transwell migration assays (**H**) were conducted with these cells. **I, J** HBP1 protein expression (**I**) and transwell assays (**J**) of FBL-3 cells stably expressing Ctrl or shHbp1-1 or shHbp1-2 after miR-29c/b2 inhibitor or a scrambled inhibitor infection. **K** Representative images of IHC of HBP1 in BM of miR-29c&b2^{-/-} mice or WT mice with virus-derived AML and quantitative analysis of HBP1 intensity in BM. All results are representative of at least three independent experiments.

Table 1 The most differentially expressed genes in bone marrow between WT and miR-29c&b2^{-/-} mice.

Gene id	Gene name	P value
ENSMUSG00000096929	A330023F24Rik	8.60E-13
ENSMUSG00000099519	Gm29253	1.21E-11
ENSMUSG00000029657	Hsph1	3.81E-11
ENSMUSG00000031762	Mt2	5.29E-07
ENSMUSG00000020900	Myh10	1.26E-06
ENSMUSG00000053846	Lipg	1.59E-06
ENSMUSG00000034480	Diap2	1.07E-05
ENSMUSG00000026411	Tmem9	2.93E-05
ENSMUSG00000027562	Car2	4.44E-05
ENSMUSG00000041329	Atp1b2	4.47E-05
ENSMUSG00000102748	Pcdhgb2	4.41E-05
ENSMUSG00000006567	Atp7b	5.85E-05
ENSMUSG00000024939	Fam89b	8.19E-05
ENSMUSG00000041570	Camsap2	7.13E-05
ENSMUSG00000046959	Slc26a1	5.65E-05
ENSMUSG00000059108	Ifitm6	7.57E-05
ENSMUSG00000067149	Jchain	7.57E-05
ENSMUSG00000068105	Tnfrsf13c	8.30E-05
ENSMUSG00000071796	6820431F20Rik	6.37E-05

AML patients with liver or splenomegaly expressed high miR-29c&b2 and MYH10 with low HBP1

To explore the relationship between HBP1/MYH10 and the prognosis of AML patients, we analyzed the TCGA database. Compared to a favorable group, which categorized by

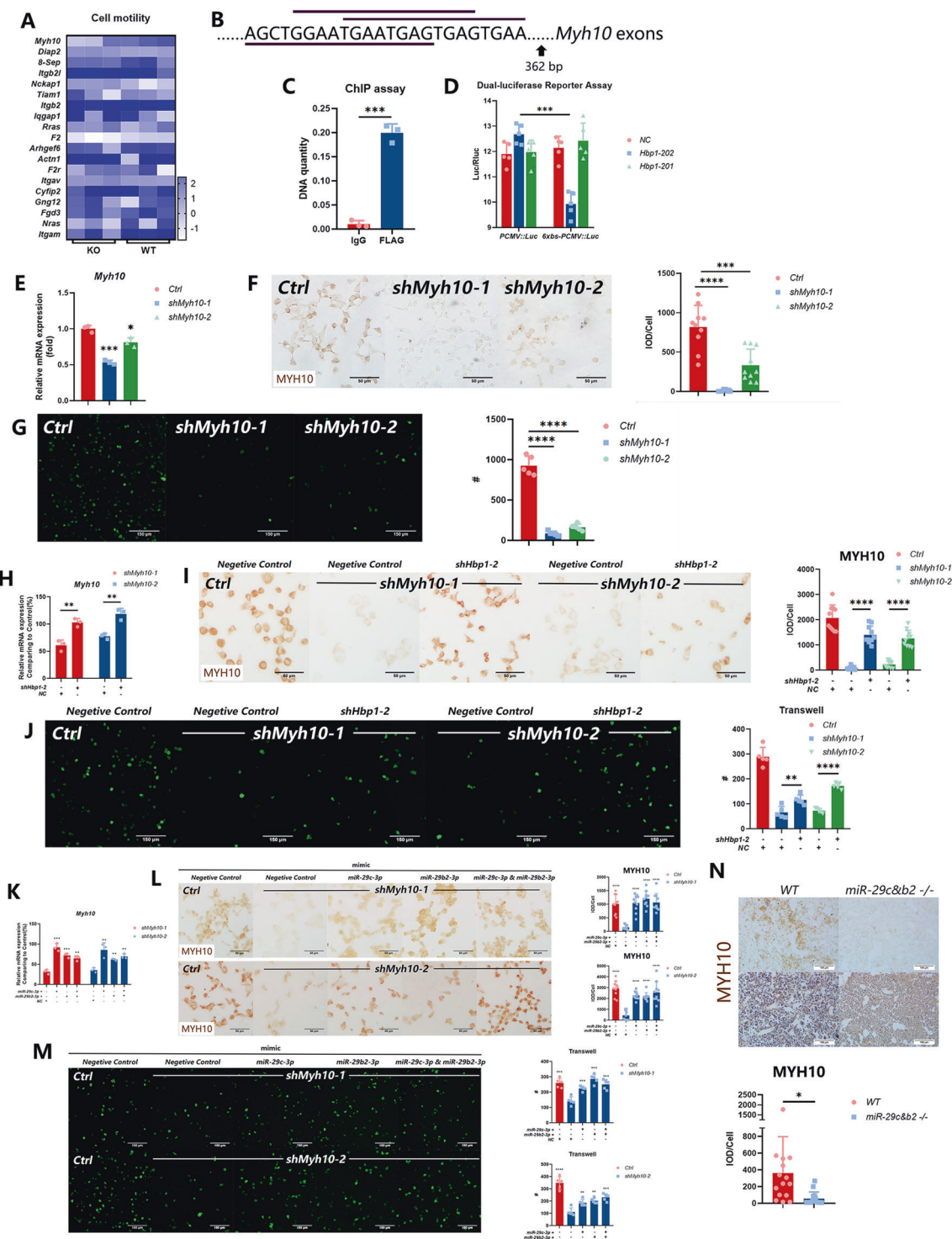
CALGB cytogenetics risk category, patients in the poor risk group had lower HBP1 and higher MYH10 (Fig. 5A). In addition, we observed an increased expression of miR-29c&b2 in primary AML patients with liver or splenomegaly compared to those without these conditions (Fig. 5B and Table 3). Lower HBP1 and higher MYH10 were then confirmed by testing specimens of AML patients with liver or splenomegaly on both RNA and protein levels (Fig. 5B–D and Table 3). These observations provided convincing in vivo evidence of an inverse relationship between the prognosis of AML patients and miR-29c&b2, which could be resulted from encouraging the EMI by regulating HBP1/MYH10 axis (Fig. 5E).

Discussion

Several clinical studies have found that EMI is associated with low complete remission rate and poor prognosis in AML [6, 8–10]. However, the mechanism of EMI remains indistinct. We found that miR-29c&b2 promoted the invasion of AML cells and encouraged the EMI by regulating cells motility.

In AML, liver or splenomegaly is one of the most common EMI events and can be diagnosed by computerized tomography scan or ultrasonography. Though EMI is more frequent in subtype M4 or M5, research shows that it remains as an independent poor risk factor in all subtypes of AML [6]. Meanwhile, over 50% of deceased AML patients are reported to have multi-system extramedullary leukemia infiltration at their death [23–25]. As reported, miR-29 family may play a vital role in AML. Interestingly, miR-29a has been reported to relate to the good outcome of AML [26] while miR-29c&b2 are related to the poor outcome [14], even though all of them share the same seed sequence. In addition, many studies on miR-29a&b1 in AML, ranging from apoptosis and proliferation, have suggested that miR-29a&b1 work as a tumor suppressor in AML [12, 13]. Meanwhile, miR-29c&b2 may perform as an oncogene in AML by encouraging EMI, which is why we are interested in exploring and confirming their exact effect in AML.

In both mice and AML patients' specimens, we found that higher miR-29c&b2 resulted in more severe cases of EMI. Our experiments in vitro also showed that higher miR-29c&b2 was associated with increased migration of leukemia cells. Meanwhile, other studies have also reported that miR-29s can promote tumor metastasis in both breast cancer and pancreatic cancer [27–29]. Interestingly, our studies showed that miR-29c&b2 was associated with lighter BM leukemia burden in vivo, which was aligned with information from the TCGA database. Although the homing of leukemia cells was decreased by the miR-29c&b2 loss, the leukemia burden in marrow of miR-29c&b2^{-/-} AML



models was heavier, which may be resulted from the enhanced proliferation and decreased apoptosis by miR-29c&b2 loss. Recent studies on miR-29s' role in inhibiting proliferation and promoting apoptosis by CDK6, DNMT3B, MCL1 may explain the results above [30–33]. And the suppressed invasion ability of leukemia cells by miR-29c&b2 loss was responsible for the mismatching leukemia

burden in BM and PB. Moreover, studies on solid tumors usually regard proliferation and metastasis as two different routes in tumor cells' evolution and mutually exclusive in most cases. For example, low-expression E-cadherin and FBXO22 are associated with high invasiveness and low proliferation, and result in poor outcome in breast cancer [34–36]. Therefore, we speculated that miR-29c&b2 might

◀ **Fig. 4 Hbp1 mediates the transcription of Myh10.** **A** Differential genes in cell motility by RNA-seq analysis of c-Kit⁺ cells in BM of the WT and miR-29c&b2^{-/-} mice. **B** Three predicted Hbp1 binding sites in Myh10 promoter. **C** FBL-3 cells stably expressing FLAG-Hbp1 were subjected to ChIP-PCR assay. **D** Luciferase expression in 293T cells transfected with pmirGLO-REPORTTM vector or which containing 6xbs and transfected with eGFP-N1 vector or Hbp1-202/201-eGFP-N1 vector. Renilla luciferase activity was used as a reference. **E–G** Myh10 RNA (**E**) or protein (**F**) expression of FBL-3 stably expressing Ctrl or shMyh10-1 or shMyh10-2. Transwell migration assays (**G**) were conducted with these cells. **H–J** Myh10 RNA (**H**) or protein (**I**) expression or transwell assays (**J**) of FBL-3 cells stably expressing Ctrl or shMyh10-1 or shMyh10-2 after Ctrl or shHbp1-2 lentivirus infected. **K–M** Myh10 RNA (**K**) or protein (**L**) expression or transwell assays (**M**) of FBL-3 cells stably expressing Ctrl or shMyh10-1 or shMyh10-2 after miR-29c/b2-3p mimic or a scrambled mimic infection. **N** Representative images of IHC of MYH10 in BM of miR-29c&b2^{-/-} mice or WT mice with virus-derived AML and quantitative analysis of MYH10 intensity in BM. All results are representative of at least three independent experiments.

work as a double-edged sword, but their primary role is promoting EMI in AML, which results in poor prognosis.

The miR-29s family consists of four members, 29a&b1 and 29c&b2, located on two different chromosomes sharing the same seed sequence [37]. The predicted target genes of miR-29c&b2 ranged widely in multiple pathways. Three datasets of predicted target genes were cross-compared to narrow down the possible genes in our works. We identified several potential target genes of miR-29c/b2 that were reported regulating cell invasion or migration, including HBP1, ADAMTS17, SPARC, and BACH2 [38–41]. The expression of ADAMTS17, SPARC, and BACH2 were not related to the prognosis of AML according to the survival analysis in TCGA (data not shown). Meanwhile, HBP1, as an HMG-box transcription inhibitor, usually inhibits gene expression by isolating other transcription factors or collecting co-factors [42]. It was reported lower HBP1 in AML LSC comparing to AML non LSC [43]. The survival analysis also demonstrated that low expression of HBP1 was related to a poor outcome in AML in our study. Thus, we preferred to focus on HBP1 as a primary downstream target of miR-29c&b2. Other researches show that HBP1 can be regulated by several miRNAs, such as miR-155, miR-21, miR-17, or miR-96 [44–46]. miR-29a is also proved to target HBP1 in human endothelial cells and hematopoietic stem cell [43, 47]. Furthermore, it has been reported that the reduction of HBP1 can promote the migration ability of lung cancer cells and relates to invasive breast cancer [40, 48]. Our study found that HBP1 was regulated by miR-29c&b2, the suppression of which could promote the migration of leukemia cells.

In addition, we were the first to report that Hbp1 could suppress the transcription of Myh10 directly. Due to the decrease of Hbp1 expression, the transcription of Myh10 increased, which also caused the enhancement of cell

migration. Physical descriptions of cell migration usually involve front protrusion, adhesion, contraction, and rear detachment that lead to forward motion in a polarized cell [49]. Myosin motors are key factors in protrusion and contraction by dynamic self-assembly and force-generating properties. Myosin, widely found in non-myoblasts, is a component of the cytoskeleton that provides the necessary force for cytoplasm flow, cytogenetic movement, material transport, filament division, cytoplasm division, and cell top growth [50]. Since myosin II motors cross-link actin filaments slide filaments and facilitate network contraction by hydrolyzing ATP, they also play a heavy role in cell migration and formation [51]. MYH10, as an important member of myosin family, is reported to play a heavy role in cell motility and cell mechanics. Studies showed that Myh10 is required for vessel formation and neuronal migration in mammal and regulates cell width and tissue angle changes during zebrafish brain morphogenesis [52, 53]. In the case of cancer cells, MYH10 can promote the metastasis of gliomas [54]. Our study was the first to reveal the role of MYH10 in AML infiltration, thereby providing a new idea for clinical therapy.

The role of miR-29c&b2 in AML was quite complex, and our studies were the first to show that the miR-29c&b2/HBP1/MYH10 signal axis played an important role in promoting EMI and leading to poor outcomes. Therefore, extra attention should be given to AML patients with related genes expression due to the possibility of MRD in extramedullary organs. However, it remains unknown whether there are other pathways regulated by miR-29c&b2 in EMI and the value of miR-29c&b2 in new therapy also needs further exploration.

Method

Patients specimens and TCGA dataset

Twenty BM samples from patients with AML of Shanghai Ninth People's Hospital were retrospectively selected for this study and were reviewed by pathologists to confirm the diagnosis according to the criteria described by the 2016 World Health Organization classification for hematopoietic diseases based on morphological criteria. The inclusion criteria for this study were the availability of BM, patient age no less than 18 years, and available clinical and demographic data. This study was approved by the local Ethics in Research Committee. All the patients signed the written informed consent form before enrolled in this study. According to the liver or splenomegaly or not at first diagnosis of AML, patients were divided into two groups and the BM samples were obtained before the first chemotherapy.

Table 2 Gene sets analysis.

#Term	Database	ID	Input number	Background number	Corrected <i>P</i> value	Input
Acute myeloid leukemia	KEGG PATHWAY	mmu05221	9	69	0.00527	Bc12a1d1Stat3Ccmd1Pik3cblNrasPik3r2Pml1Lef1Iltgam
Cell differentiation	Gene Ontology	GO:0030154	63	1004	3.90E-06	Bmp8b1Tal1Lrrk2HeylItgav1Gm14490IPkdcc1Cbfa2t3Vegfb1Hck1Calr3Klh10Spib1Sik1Ntng2IDdx25Ccdc36Foxo1Fgr1Cplx2Spag8Slco4c1Hes1Rho1Hspa1Gata2Ccdc85b1Nr1h3Pax5Smurf1Tnfsf1Ptkt2Fam65bSfrp4Tex15Syne1Nhs12Robo4Hemgn1Bmpr1a1Rasgrp4Mycbpap1Sort1Sema4a1Ngfr1Sema4f1Rmdn3Bmp7Corin1Rasgrp1Bmp1Fam210b1Bhlhe41Sox12Zfp11Rfx2Nr1i3Rbm24Ets1Diap2InalGas7Abhd5
Positive regulation of erythrocyte differentiation	Gene Ontology	GO:0045648	8	27	0.000158	Stat3Fam210b1Acvr1b1Inhba1Ets1Tal1Gata2Gata1
Myeloid cell differentiation	Gene Ontology	GO:0030099	7	27	0.000906	Clec5a1Tal1Tirap1Cdkn1c1Prdx3Pml1Gata1

Almost 198 AML cases assayed on RNA sequencing and miRNA sequencing were included in the analysis. Sequence files are available from CGHub (<https://cghub.ucsc.edu>). All other molecular, clinical, and pathological data are available through the TCGA Data Commons (<https://gdc.nci.nih.gov/>).

CRISPR/Cas9-mediated generation of a miR-29c&b2^{-/-} mice

Homozygous miR-29c&b2^{-/-} mice (C57BL/6 strain) were generated using the CRISPR/Cas9 technique from Shanghai Model Organisms Center, Inc (Shanghai, China). Briefly, guide RNAs (gRNAs) were designed for targeting the 5' and 3' ends of mouse miR-29c&b2 based on publicly available information on the sequences of miR-29c (miR-Base:MI0000577) and miR-29b2 (miR-Base:MI0000712). The spacer sequences of the gRNAs were as follows: gRNA1: 5'-TCTACCGACACTATGCATCT-3'; gRNA2: 5'-CTACCGACACTATGCATCTT-3'; gRNA3: 5'-AACTAAGTACTGTAAACGT-3'; and gRNA4: 5'-GCACA GCAAATTAACCTTCC-3'. A mixture of gRNA and Cas9 mRNA was microinjected into one-cell stage mouse embryos from C57BL/6 mice. The injected embryos were then implanted into pseudo-pregnant C57BL/6 mice to generate F0 mice. The F0 mice were genotyped using PCR with primers designed to anneal to the 5' and 3' ends of miR-29c&b2. These PCR-amplified products were sequenced to confirm complete deletion of miR-29c&b2. The homozygous mice (miR-29c&b2^{-/-}) were bred for at least four generations at the Shanghai Model Organisms

Center (Shanghai, China) prior to starting any experiments. The WT C57BL/6 mice were obtained from the Shanghai Model Organisms Center (Shanghai, China) and housed five per cage, fed standard laboratory chow and deionized water, according to Institutional Animal Care and Use Committees protocols.

Cell lines, culture, and treatments

FBL-3 cells, C1498 cells, and MV4-11 cells were cultured in complete RPMI 1640 medium supplemented with 10% heat-inactivated fetal bovine serum (Gibco) and maintained in a humidified atmosphere of 5% CO₂ at 37 °C. FBL-3 cell line was a gift from Henan Tumor Hospital. C1498 and MV4-11 cells were purchased from the Shanghai Model Organisms Center, Inc (Shanghai, China) and National Collection of Authenticated Cell Cultures (Shanghai, China). In this study, an absence of mycoplasma or bacterial contamination of the cells was detected. AML cells knocked out miR-29c&b2 by CRISPR/Cas9. Sequences of miR-29c&b2 sgRNAs were inserted into Lenti-sgRNA-eGFP vector. The monoclonal cells were sorted by a FACSAria Cell Sorter (BD) and identified by PCR. Cells were transfected with mimics (miR10000536-1, miR10000127-1, miR1N0000001-1, Ribobio) or inhibitors (miR20000536-1, miR20000127-1, miR2N0000001-1, Ribobio) of miR-29c-3p, miR-29b2-3p or negative control as a scramble microRNA in 48-well plates using riboFECT CP Transfection Kit (Ribobio) according to the manufacturer's instructions.

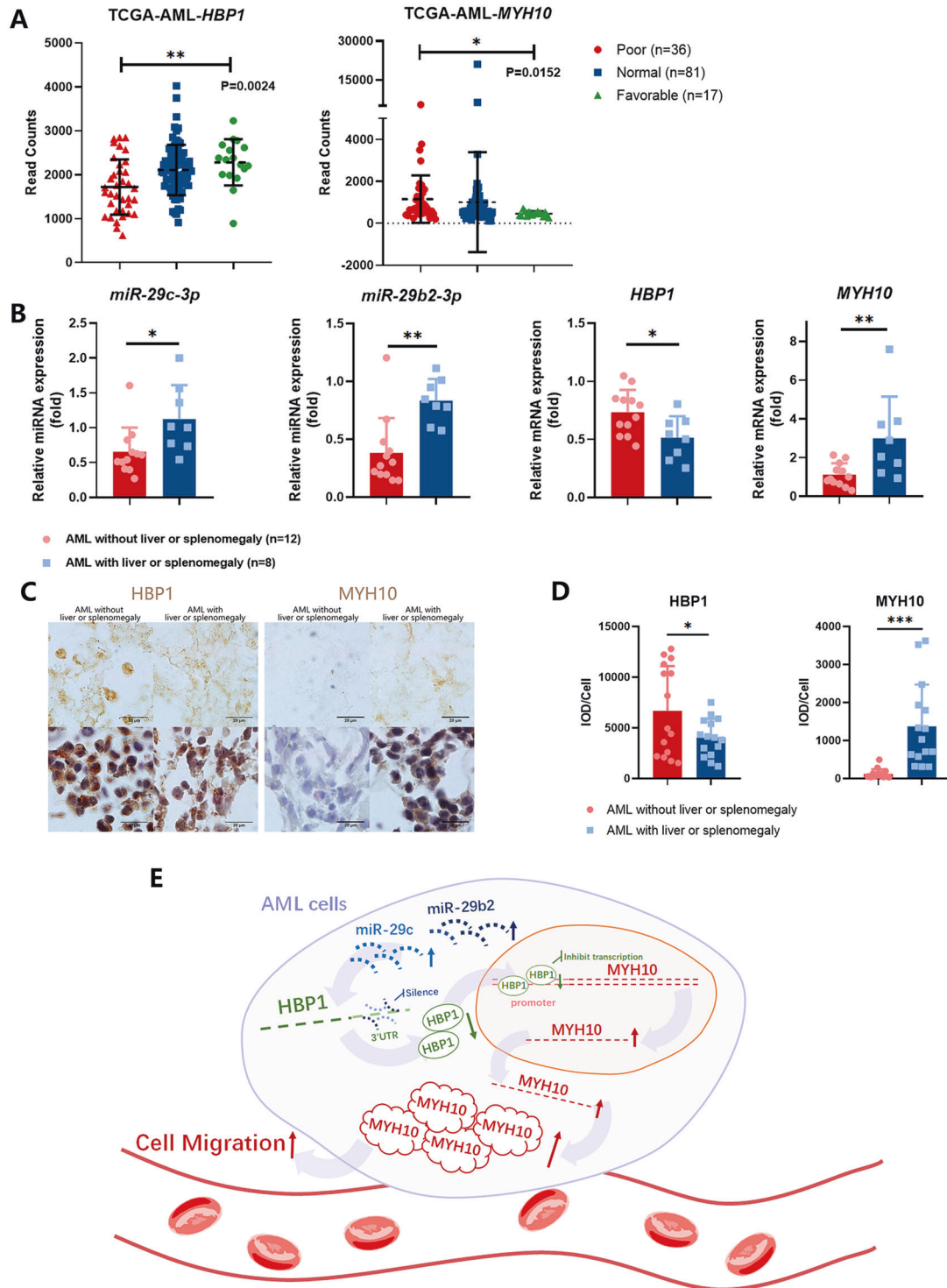


Fig. 5 AML patients with liver or splenomegaly expressed high miR-29c&b2 and MYH10 with low HBP1. **A** Patients with AML excluded subtype M3 in TCGA database was classified by CALGB cytogenetics risk category. The expression analysis of HBP1 or MYH10 was conducted. **B** The BM of AML patients with ($n = 12$) or without ($n = 8$) liver or splenomegaly were subjected to qPCR

analysis. **C** Representative images of IHC of HBP1 or MYH10 in BM of AML patients with or without liver or splenomegaly. **D** Quantitative analysis of HBP1 or MYH10 intensity in BM. **E** The schematic cartoon of the mechanism of miR-29c&b2 encouraging EMI in AML cells. All results are representative of at least three independent experiments.

Table 3 Characteristics of AML patients.

Characteristic	AML without liver or splenomegaly	AML with liver or splenomegaly
Age, years		
Median	59.1	43.5
Min–max	37–76	21–65
Gender		
Male	6	5
Female	6	3
Prior MDS		
Yes	0	0
No	12	8
Subtype		
M0	1	1
M1	2	1
M2	3	2
M4	4	2
M5	2	2
ECOG PS		
0	10	7
1	2	1
Co-occurring mutations		
CEBPA	2	0
DNMT3A	2	1
NRAS	0	1
NPM1	2	1
TET2	0	1
FLT3-ITD	1	2
BCORL1	0	1
MLL/ENL	0	1
AML1/ETO	1	0
Hematology, median (range)		
WBC, $\times 10^9/L$	20.68 (1.05–134)	57.79 (4.31–218)
Hgb, g/dL	93.44 (66–130)	70.25 (57–103)
PLT, $\times 10^9/L$	58.78 (14–120)	65.5 (18–134)

Homolog assays

In all, 3×10^6 AML GFP+ cells were transplanted into C57 mice or sub-lethally irradiated NOD-SCID mice. Femurs of the recipient mice were harvested after 20 h, and the percentages of GFP+ cells were determined by flow-cytometric analysis.

Mouse AML model by Friend-MuLV or AML cells

The Friend virus (Friend-MuLV) was generated from FBL-3 cells [20, 22]. Viral supernatant was collected after an additional 24 h of culture, percolated by 0.22 μ m Sterile

Millex filter units (SLGP033RB), pooled and prepared as single-use aliquots. Adult 6- to 8-week-old male C57 mice or sub-lethally irradiated NOD-SCID mice were injected intravenously with 100 μ l supernatant or 1×10^6 AML cells for constructing secondary AML model or AML xenograft model. Six per group of mice were set up for AML xenograft models and 25 per group of mice were set up for virus-derived secondary AML model.

Mouse tissues

Peripheral blood mononuclear cells were collected by caudal veins. BM cells were prepared by washing femurs with injection needles in PBS. Red cell lysis was performed with lysis buffer before flow-cytometric analysis. For histology, samples were fixed in 4% paraformaldehyde overnight before standard processing for paraffin-embedded tissues. Then, 10- μ m sections were stained with hematoxylin-eosin/immunohistochemistry. Blood smears were stained with a modified Wright–Giemsa stain as per standard protocols.

Flow cytometry and immunochemistry

BM or PB samples were processed using a whole blood lysis technique. The immunophenotyping was performed by multiparameter flow cytometry (EPICSTM XL-MCL, Beckman Coulter). The leukemic blasts were stained and analyzed with CD71-PE, c-Kit-PE-Cy7 (113807, 105814, Biolegend). The paraffin sections of mice tissues were dewaxed, antigen retrieval and blocked with 5% BSA as per standard protocols. Sections were stained using the polyclonal antibodies c-Kit (ab25022, abcam) or GFP (50430-2-AP, Proteintech).

Dual-luciferase reporter analysis

For luciferase reporter assays, HEK293T cells were seeded in 96-well plate 24 h before plasmid transfection. The miR-29c&b2-3p mimics/inhibitors (miR10000536-1, miR10000127-1, miR1N0000001-1, miR20000536-1, miR20000127-1, miR2N0000001-1, Ribobio) with pmirGLO-REPORT™ vectors (Hbp1 3'UTR WT or Mut) were co-transfected into cells using lipofectamine 2000. For Myh10 promoter activity assay, six repeats of the predicted binding site were cloned and inserted before the CMV promoter in pmirGLO-REPORT™ vector. Sequence of Hbp1-202 (NM_153198.3) and Hbp1-201 with lacking HMG-box domain (NM_177993.4) were cloned into pGFP-N1 vector. HEK293T cells were co-transfected with pGFP-FLAG-Hbp1-202/201-N1 vectors (NM_177993.4; NM_153198.3) and pmirGLO-6xbs-REPORT™ vector. Cells were harvested 48 h later and assayed using Dual-Luciferase Reporter Assay System (Beyotime). Renilla luciferase activity was used as a reference.

Cell migration and transwell assays

The culture medium with 20% FBS was added in under chamber. Cells were suspended with culture medium with serum free and then seeded (5×10^3 cells) in the top chamber of transwell plate. After 6 h, the chambers were removed and cells in the plates were counted under microscope at five fields per filter.

Cell viability and differentiation analysis

Cell viability was determined using a CCK-8 assay kit (Beyotime) according to the manufacturer's instructions. Clones formation assays were conducted with soft agar. The differentiation analyses were evaluated by flow cytometry with CD71-PE (113807, Biolegend), CD11b-APC-Cy7 (557657, BD), CD14-APC (301808, Biolegend), and CD11b-PE (555388, BD).

Isolation and expression analysis of microRNAs or mRNAs

Total RNA was extracted from collected AML mononuclear cells using Trizol (Sigma) according to the protocol of the manufacturer. cDNA synthesis was performed on 2 µg of RNA using miRcute Plus miRNA First-Strand cDNA Kit (KR211) or TIANGEN Script II RT Kits (TIANGEN KR107). Quantitative real-time PCR was performed using the SuperReal PreMix Plus (SYBR Green) (TIANGEN FP205). The expression levels of relative genes were calculated and quantified by using the $\Delta\Delta C_t$ method after normalization by expression of endogenous control.

Protein expression analysis

To verify protein expression levels, western blotting assays were performed by using the following antibodies: polyclonal anti-HBP1 (11746-1-AP, Proteintech) and polyclonal anti- β -actin (ab8227, abcam). After exposure to ECL Prime (Beyotime), blots were developed using the c-Digit imaging system (ImageQuant LAS 4000mini). Immunohistochemical (IHC) was performed in accordance with well-established protocols. The primary antibodies for IHC were polyclonal anti-MYH10 (8824, CST) or polyclonal anti-HBP1 (11746-1-AP, Proteintech). Tissue sections were then incubated with secondary Goat Anti-Rabbit (HRP) antibody (ab7090, abcam) and HRP activity was visualized using the DAB (Beyotime) according to the manufacturer's instructions. Tissue sections were then dehydrated and mounted with a coverslip using neutral resins (Solarbio).

Chromatin immunoprecipitation assay

FBL-3 were infected with lentivirus and overexpressed 3 \times FLAG-Hbp1-202 protein. Then cells were collected and crosslinked with 1% formaldehyde and lysed in SDS lysis buffer, sheared with ChIP-IT[®] Express Enzymatic Shearing Kit (ActiveMotif). The antibody against FLAG (14793, CST) or Normal Rabbit IgG (2729, CST) was then added to the supernatant, incubated overnight at 4 °C with rotation and incubated with 100 µL Salmon Sperm DNA/Protein A agarose beads for 2 h at 4 °C. Then, the immunoprecipitated complex was washed and eluted. The DNA crosslinks were reversed, and DNA was purified for real-time PCR.

Statistical analysis

The significance of the differences between the groups was determined with an ANOVA test or Student's *t* test, and $P < 0.05$ was considered statistically significant. The results were expressed as the mean \pm SD from at least three independent experiments. Kaplan–Meier method was used to calculate overall survivals, and the differences were analyzed by a log-rank test.

Acknowledgements This study was supported by the National Natural Science Foundation of China (No. 81870132, 81261120568) and the Science and Technology Commission of Shanghai Municipality (18DZ2290700, 18DZ2293500).

Compliance with ethical standards

Conflict of interest The authors declare no competing interests.

Ethics approval and consent to participate All human bone marrow specimens were collected from patients diagnosed with AML at the Shanghai Ninth People's Hospital, China, from 2016 to 2020. Informed consent was obtained from all patients and the project was approved by the Ethics Committee of Shanghai Ninth People's Hospital. Six- to eight-week-old C57BL/6 or miR-29c&b2 knockout C57BL/6 mice were purchased from the Shanghai Model Organisms Center, Inc (Shanghai, China). Six- to eight-week-old NOD-SCID mice were purchased from Shanghai SLAC Laboratory Animal Co., Ltd (Shanghai, China). All experiments with mice were performed strictly in accordance with a protocol approved by the Administrative Panel on Laboratory Animal Care of the Shanghai Ninth People's Hospital.

Publisher's note Springer Nature remains neutral with regard to jurisdictional claims in published maps and institutional affiliations.

References

- Dohner H, Estey E, Grimwade D, Amadori S, Appelbaum FR, Buchner T, et al. Diagnosis and management of AML in adults: 2017 ELN recommendations from an international expert panel. *Blood*. 2017;129:424–47.
- Estey EH. Acute myeloid leukemia: 2019 update on risk-stratification and management. *Am J Hematol*. 2018;93:1267–91.

3. Junge A, Bacher U, Mueller BU, Keller P, Solenthaler M, Pabst T. Adverse outcome of AML with aberrant CD16 and CD56 NK cell marker expression. *Hematol Oncol*. 2018. [Online ahead of print].
4. Patel SS, Kuo FC, Gibson CJ, Steensma DP, Soiffer RJ, Alyea EP, et al. High NPM1-mutant allele burden at diagnosis predicts unfavorable outcomes in de novo AML. *Blood*. 2018;131:2816–25.
5. Byrd JC, Mrozek K, Dodge RK, Carroll AJ, Edwards CG, Arthur DC, et al. Pretreatment cytogenetic abnormalities are predictive of induction success, cumulative incidence of relapse and overall survival in adult patients with de novo acute myeloid leukemia. *Blood*. 2002;100:4325–36.
6. Chang H, Brandwein J, Yi QL, Chun K, Patterson B, Brien B. Extramedullary infiltrates of AML are associated with CD56 expression, 11q23 abnormalities and inferior clinical outcome. *Leuk Res*. 2004;28:1007–11.
7. Grimwade D, Walker H, Oliver F, Wheatley K, Harrison C, Harrison G, et al. The importance of diagnostic cytogenetics on outcome in AML: analysis of 1,612 patients entered into the MRC AML 10 trial. *Blood*. 1998;92:2322–33.
8. Zhou T, Bloomquist MS, Ferguson LS, Reuther J, Marcogliese AN, Elghetany MT, et al. Pediatric myeloid sarcoma: a single institution clinicopathologic and molecular analysis. *Pediatr Hematol Oncol*. 2020;37:76–89.
9. Hu GH, Lu AD, Jia YP, Zuo YX, Wu J, Zhang LP. Prognostic impact of extramedullary infiltration in pediatric low-risk acute myeloid leukemia: a retrospective single-center study over 10 years. *Clin Lymphoma Myeloma Leuk*. 2020;20:e813–20.
10. Kobayashi R, Tawa A, Hanada R, Horibe K, Tsuchida M, Tsukimoto I, et al. Extramedullary infiltration at diagnosis and prognosis in children with acute myelogenous leukemia. *Pediatr Blood Cancer*. 2007;48:393–8.
11. Xu J, Zhang W, Yan XJ, Lin XQ, Li W, Mi JQ, et al. DNMT3A mutation leads to leukemic extramedullary infiltration mediated by TWIST1. *J Hematol Oncol*. 2016;9:106.
12. Garzon R, Heaphy CE, Havelange V, Fabbri M, Volinia S, Tsao T, et al. MicroRNA 29b functions in acute myeloid leukemia. *Blood*. 2009;114:5331–41.
13. Gong JN, Yu J, Lin HS, Zhang XH, Yin XL, Xiao Z, et al. The role, mechanism and potentially therapeutic application of microRNA-29 family in acute myeloid leukemia. *Cell Death Differ*. 2014;21:100–12.
14. Butrym A, Rybka J, Baczynska D, Poreba R, Kuliczowski K, Mazur G. Clinical response to azacitidine therapy depends on microRNA-29c (miR-29c) expression in older acute myeloid leukemia (AML) patients. *Oncotarget*. 2016;7:30250–7.
15. Li Y, Cai BL, Shen LL, Dong Y, Lu Q, Sun SK, et al. MiRNA-29b suppresses tumor growth through simultaneously inhibiting angiogenesis and tumorigenesis by targeting Akt3. *Cancer Lett*. 2017;397:111–9.
16. Xu WW, Li B, Guan XY, Chung SK, Wang Y, Yip YL, et al. Cancer cell-secreted IGF2 instigates fibroblasts and bone marrow-derived vascular progenitor cells to promote cancer progression. *Nat Commun*. 2017;8:14399.
17. Zhu J, Xiong G, Fu H, Evers BM, Zhou BP, Xu R. Chaperone Hsp47 drives malignant growth and invasion by modulating an ECM gene network. *Cancer Res*. 2015;75:1580–91.
18. Zhu LH, Miao XT, Wang NY. Integrated miRNA-mRNA analysis of Epstein-Barr virus-positive nasopharyngeal carcinoma. *Genet Mol Res*. 2015;14:6028–36.
19. Ambros V. The functions of animal microRNAs. *Nature*. 2004;431:350–5.
20. Chen W, Qin H, Chesebro B, Cheever MA. Identification of a gag-encoded cytotoxic T-lymphocyte epitope from FBL-3 leukemia shared by Friend, Moloney, and Rauscher murine leukemia virus-induced tumors. *J Virol*. 1996;70:7773–82.
21. Dawson PJ, Fieldsteel AH, Bostick WL. Pathologic studies of Friend virus leukemia and the development of a transplantable tumor in BALB/c mice. *Cancer Res*. 1963;23:349–54.
22. De Harven E, Friend C. Further electron microscope studies of a mouse leukemia induced by cell-free filtrates. *J Biophys Biochem Cytol*. 1960;7:747–52.
23. Liu JH, Zhou F, ZX L, Zhang SF. Pathological findings of multi-organ invasion during autopsy of 101 patients with acute leukemia. *Chin J Practical Intern Med*. 2014;034:1112–3.
24. Thiele J, Laubert A, Vykoupil KF, Georgii A. Autopsy and clinical findings in acute leukemia and chronic myeloproliferative diseases-an evaluation of 104 patients. *Pathol Res Pr*. 1985;179:328–36.
25. Viadana E, Bross ID, Pickren JW. An autopsy study of the metastatic patterns of human leukemias. *Oncology*. 1978;35:87–96.
26. Zhu C, Wang Y, Kuai W, Sun X, Chen H, Hong Z. Prognostic value of miR-29a expression in pediatric acute myeloid leukemia. *Clin Biochem*. 2013;46:49–53.
27. Cochrane DR, Jacobsen BM, Connaghan KD, Howe EN, Bain DL, Richer JK. Progesterone regulated miRNAs that mediate progesterone receptor action in breast cancer. *Mol Cell Endocrinol*. 2012;355:15–24.
28. Rostas JW III, Pruitt HC, Metge BJ, Mitra A, Bailey SK, Bae S, et al. microRNA-29 negatively regulates EMT regulator N-myc interactor in breast cancer. *Mol Cancer*. 2014;13:200.
29. Sun XJ, Liu BY, Yan S, Jiang TH, Cheng HQ, Jiang HS, et al. MicroRNA-29a promotes pancreatic cancer growth by inhibiting tristetrapirolin. *Cell Physiol Biochem*. 2015;37:707–18.
30. Fabbri M, Garzon R, Cimmino A, Liu Z, Zanesi N, Callegari E, et al. MicroRNA-29 family reverts aberrant methylation in lung cancer by targeting DNA methyltransferases 3A and 3B. *Proc Natl Acad Sci USA*. 2007;104:15805–10.
31. Mott JL, Kobayashi S, Bronk SF, Gores GJ. miR-29 regulates Mcl-1 protein expression and apoptosis. *Oncogene*. 2007;26:6133–40.
32. Robaina MC, Mazzoccoli L, Arruda VO, Reis FR, Apa AG, de Rezende LM, et al. Deregulation of DNMT1, DNMT3B and miR-29s in Burkitt lymphoma suggests novel contribution for disease pathogenesis. *Exp Mol Pathol*. 2015;98:200–7.
33. Zhao JJ, Lin JH, Lwin T, Yang H, Guo JP, Kong W, et al. microRNA expression profile and identification of miR-29 as a prognostic marker and pathogenetic factor by targeting CDK6 in mantle cell lymphoma. *Blood*. 2010;115:2630–9.
34. Hugo HJ, Gunasinghe N, Hollier BG, Tanaka T, Blick T, Toh A, et al. Epithelial requirement for in vitro proliferation and xenograft growth and metastasis of MDA-MB-468 human breast cancer cells: oncogenic rather than tumor-suppressive role of E-cadherin. *Breast Cancer Res*. 2017;19:86.
35. Padmanaban V, Krol I, Suhail Y, Szczerba BM, Aceto N, Bader JS, et al. E-cadherin is required for metastasis in multiple models of breast cancer. *Nature*. 2019;573:439.
36. Sun R, Xie HY, Qian JX, Huang YN, Yang F, Zhang FL, et al. FBXO22 possesses both protumorigenic and antimetastatic roles in breast cancer progression. *Cancer Res*. 2018;78:5274–86.
37. Kwon JJ, Factora TD, Dey S, Kota J. A systematic review of miR-29 in cancer. *Mol Ther Oncolytics*. 2019;12:173–94.
38. Chen X, Yue B, Zhang C, Qi M, Qiu J, Wang Y, et al. MiR-130a-3p inhibits the viability, proliferation, invasion, and cell cycle, and promotes apoptosis of nasopharyngeal carcinoma cells by suppressing BACH2 expression. *Biosci Rep*. 2017;37:BSR20160576.
39. Le Goff C, Cormier-Daire V. The ADAMTS(L) family and human genetic disorders. *Hum Mol Genet*. 2011;20:R163–7.
40. Paulson KE, Rieger-Christ K, McDevitt MA, Kuperwasser C, Kim J, Unanue VE, et al. Alterations of the HBP1 transcriptional repressor are associated with invasive breast cancer. *Cancer Res*. 2007;67:6136–45.

41. Qu X, Gao D, Ren Q, Jiang X, Bai J, Sheng L. miR-211 inhibits proliferation, invasion and migration of cervical cancer via targeting SPARC. *Oncol Lett.* 2018;16:853–60.
42. Bollaert E, Serra AD, Demoulin JB. The HMG box transcription factor HBP1: a cell cycle inhibitor at the crossroads of cancer signaling pathways. *Cell Mol Life Sci.* 2019;76:1529–39.
43. Han YC, Park CY, Bhagat G, Zhang J, Wang Y, Fan JB, et al. microRNA-29a induces aberrant self-renewal capacity in hematopoietic progenitors, biased myeloid development, and acute myeloid leukemia. *J Exp Med.* 2010;207:475–89.
44. Sun X, Geng X, Zhang J, Zhao H, Liu Y. miR-155 promotes the growth of osteosarcoma in a HBP1-dependent mechanism. *Mol Cell Biochem.* 2015;403:139–47.
45. Wu H, Ng R, Chen X, Steer CJ, Song G. MicroRNA-21 is a potential link between non-alcoholic fatty liver disease and hepatocellular carcinoma via modulation of the HBP1-p53-Srebp1c pathway. *Gut.* 2016;65:1850–60.
46. Yan Z, Wang J, Wang C, Jiao Y, Qi W, Che S. miR-96/HBP1/Wnt/ β -catenin regulatory circuitry promotes glioma growth. *FEBS Lett.* 2014;588:3038–46.
47. Yang Z, Wu L, Zhu X, Xu J, Jin R, Li G, et al. MiR-29a modulates the angiogenic properties of human endothelial cells. *Biochem Biophys Res Commun.* 2013;434:143–9.
48. Su CY, Cheng X, Li YS, Han Y, Song XY, Yu DP, et al. MiR-21 improves invasion and migration of drug-resistant lung adenocarcinoma cancer cell and transformation of EMT through targeting HBP1. *Cancer Med.* 2018;7:2485–503.
49. Lackie JM. Crawling movement. *Cell movement and cell behaviour.* Berlin: Springer Netherlands. 1986. pp 145–74.
50. Robert-Paganin J, Pylypenko O, Kikuti C, Sweeney HL, Houdusse A. Force generation by myosin motors: a structural perspective. *Chem Rev.* 2020;120:5–35.
51. Kiani FA, Fischer S. Catalytic strategy used by the myosin motor to hydrolyze ATP. *Proc Natl Acad Sci USA.* 2014;111:E2947–56.
52. Gutzman JH, Sahu SU, Kwas C. Non-muscle myosin IIA and IIB differentially regulate cell shape changes during zebrafish brain morphogenesis. *Dev Biol.* 2015;397:103–15.
53. Ridge LA, Mitchell K, Al-Anbaki A, Qureshi WMS, Stephen LA, Tenin G, et al. Non-muscle myosin IIB (Myh10) is required for epicardial function and coronary vessel formation during mammalian development. *Plos Genet.* 2017;13:e1007068.
54. Wang Y, Yang Q, Cheng Y, Gao M, Kuang L, Wang C. Myosin heavy chain 10 (MYH10) gene silencing reduces cell migration and invasion in the glioma cell lines U251, T98G, and SHG44 by inhibiting the Wnt/ β -Catenin pathway. *Med Sci Monit.* 2018;24:9110–9.